sustainability

MDPI

Article

Chitosan-Loaded Copper Oxide Nanoparticles: A Promising Antifungal Nanocomposite against Fusarium Wilt Disease of Tomato Plants

Mohamed A. Mosa * and Sozan E. El-Abeid

Nanotechnology & Advanced Nano-Materials Laboratory (NANML), Mycology and Disease Survey Research Department, Plant Pathology Research Institute, Agricultural Research Center, Giza 12619, Egypt; sozanelabeid@yahoo.com

* Correspondence: mohammed_sharouny@yahoo.com; Tel.: +20-101-827-4608

Abstract: The extensive use of agrochemicals for crop protection is increasing their environmental risks. Due to the incredible antimicrobial potential of nanomaterials, research into their potential use in sustainable agriculture as alternatives to chemical fungicides is advancing rapidly. In this study, we evaluated the possible antifungal properties of copper oxide nanocomposite (CH@CuO NPs) coated with chitosan in order to fend off Fusarium wilt diseases in tomato plants caused by *F. oxysporum f.* sp. *lycopersici* (FOL) throughout in vitro and in vivo experiments. Here, we demonstrate some of the characteristics of a potential antifungal nanocomposite composed of copper oxide nanoparticles (CuO NPs), firmly immobilized on chitosan nanoparticle (CH) surfaces as dark spots, with an irregular shape and 54.22 nm in size, as indicated by Transmission electron microscope (TEM) analysis. Spectroscopic and microscopic investigations, as well as its antifungal efficacy, verified that the successful synthesis of the CH@CuO NPs at three different concentrations (1, 25, and 50) mg/L against three different wild isolates of the pathogenic *Fusarium oxysporum* that infect tomatoes was successfully proven to be effective. In vitro comparisons revealed that CH@CuO NPs showed stronger antifungal activity at only 1 mg/L (96.22 ± 1.35) than the classical chemical fungicide "Kocide 2000" at conc. 2.5 g/L (77.34 ± 0.33), for example, in the case of FOL1 isolate. In accordance with the in vivo data, tomato plants can be treated with only 1 mg/L of CH@CuO NPs for up to 75 days, by which time Fusarium wilt disease severity is reduced by 91.5% In contrast, 2.5 g/L of Kocide 2000 is required to reduce disease in tomato plants by about 90%. This research expands our understanding of agro-nanotechnology by outlining the characteristics of a unique, environmentally friendly, and economically viable nanopesticide for long-term plant protection.

Keywords: chitosan; copper oxide; tomato; Fusarium wilt; *Fusarium oxysporum*

Citation: Mosa, M.A.; El-Abeid, S.E. Chitosan-Loaded Copper Oxide Nanoparticles: A Promising Antifungal Nanocomposite against Fusarium Wilt Disease of Tomato Plants. *Sustainability* **2023**, *15*, 14295. https://doi.org/10.3390/su151914295

Academic Editor: Harvey Hou

Received: 16 August 2023
Revised: 23 September 2023
Accepted: 25 September 2023
Published: 27 September 2023

1. Introduction

Tomato (*Solanum lycopersicum*) is an important horticultural product grown at nearly all latitudes and is one of the world's most extensively cultivated vegetable crops, which is recognized for its significant nutritional content (http://www.fao.org/ accessed on 5 November 2022). According to [1], tomatoes are cultivated on approximately 4 million hectares of arable land, yielding over one hundred million tonnes of total production worth about USD 5–6 billion. In terms of annual output, Egypt ranks in the top ten tomato-growing countries, with about 181,000 hectares dedicated to the crop [1]. It was estimated that more than 200 diseases are responsible for 70–95% of annual global tomato crop losses [2]. Fusarium wilt disease is a significant threat to vegetable production around the world [3,4]. Vascular wilt syndrome is a deadly disease caused by the pathogenic fungus *Fusarium oxysporum* that attacks members of the family solanaceae including tomatoes [5]. Because it can survive in the soil for longer than twenty years, it is among one of the

most devastating soil-borne fungi in the globe, and *F. oxysporum* impacts crops like pepper, tomato, and potatoes. There are currently about 120 different strains of *F. oxysporum*, known as formae speciales, and each one is very specific to the host on which it triggers the disease [6]. Fusarium wilt, induced by *F. oxysporum f.* sp. *lycopersici* (FOL) on tomato plants, ranks as one of the most prevalent fungal diseases in the majority of African and Asian Mediterranean nations [7]. Certain plant fungal diseases, such as Fusarium wilt, are effectively managed with copper-based biocides. [8]. However, the development of resistance in disease-causing organisms due to prolonged exposure to these substances is never a good thing. Many kinds of fungicides are unable to control *Fusarium oxysporum* strains that infect different crops including tomatoes. Therefore, there is an urgent need for the development of innovative ways that are effective and risk-free in protecting tomatoes from Fusarium diseases. Metal oxides and inorganic nano-biocides have recently garnered attention as promising alternatives to conventional fungicides for managing plant diseases, e.g., CuO [9], ZnO [10], and MgO and TiO_2 [10,11]. Research for safe and cost-effective substitutes has continued [12,13], even though silver (Ag)-based nanocomposites and other different non-metallic nanoparticles have exhibited substantial antifungal or antibacterial activity against a variety of plant diseases [14,15]. Following this goal, scientists have published research on the promising antimicrobial activities of copper-based nano-compounds against important phytopathogenic fungi [16,17]. Copper nanoparticles (Cu NPs) and their oxides (e.g., CuO NPs) have been identified as a nutritional supplement capable of enhancing plant defense processes and stimulating plant development in *Vigna radiata* and maize [18,19]. According to [20], the antimicrobial effect of pure Cu NPs is inhibited by their tendency to aggregate. In order to address this issue, copper oxide nanoparticles with antimicrobial properties can be situated onto a renewable nano-carrier to reduce copper agglomeration within plant tissues.

Chitosan, a biodegradable, non-toxic, and biocompatible polymer, is one of the most widely recognized and promising chemical compounds that can be utilized as a natural carrier agent for powerful agents in the management of plant diseases [21]. This unique polymer has been shown to have a specific antimicrobial activity on the development of fungal virulence factors in fungi, mycelia growth, sporulation, spore viability, and germination [22]. Chitosan molecules can be employed in agriculture to protect crops and control plant diseases [23]. Although the antimicrobial actions of chitosan have not been thoroughly studied, it has been proposed to work as a chelating agent for the nutrients and minerals that microbes require for optimal growth [24]. Chitosan's antifungal activity is known to be influenced by variables like its concentration, route of application, target microorganism, and molecular weight [25]. Chitosan's high concentration of -NH_2 and -OH groups in its molecular structure makes it a useful anchoring agent for metal nanoparticles. Copper nanoparticles have been indicated to have a unique antimicrobial activity against numerous pathogenic microbial species [26]. Cu NPs exhibit higher antibacterial activity than copper salt due to their unique feature, which is a high surface area to volume ratio [27]. Its aggregation in a pure state, however, might reduce or inhibit its antibacterial action. Recent publications indicate that adding Cu NPs to carrier drugs significantly improves their antimicrobial properties [28,29].

In our present work, we aimed to investigate if chitosan-loaded copper oxide nanoparticles (CH@CuO NPs) might control the pathogenic *F. oxysporum f.* sp. *lycopersici* (FOL), which causes tomato Fusarium wilt disease. As a result, the primary objectives of the present investigation were to (1) produce a pure nanocomposite from chitosan and copper oxide nanoparticles; (2) evaluate the antifungal properties of the produced CH@CuO NPs nanocomposite to control Fusarium wilt disease in the laboratory and greenhouse; and (3) monitor changes regarding specific physiological and biochemical features in treated tomato plants.

2. Materials and Methods

2.1. Chemical Reagents

The following materials were obtained from Sigma Aldrich (Saint Louis, MO, USA) Company: Potato dextrose agar (PDA), sodium tripoly phosphate (STPP), streptomycin sulfate, and propidium iodide. While chitosan (CH) a biopolymer with a molecular weight ranging from 190 to 370 kDa, and a degree of de-acetylation of 75% was also brought from (Merck, Darmstadt, Germany) company. A commercial national supplier was used to obtain the following products: sodium hypochlorite (NaOCl) (Merck, Darmstadt, Germany), and the chemical fungicide Kocide 2000 (Certis, Columbia, MD, USA). We also employed acetic acid (Sigma-Aldrich, Saint Louis, MO, USA), 4′-6-diamidino-2-phenyl indole (DAPI), dimethyl sulfoxide (DMSO), and propidium iodide (PI Sigma-Aldrich, Saint Louis, MO, USA). Deionized water was produced using a Milli-Q Plus system (Millipore, Milford, MA, USA).

2.2. Isolation and Culturing of the Causal Agent

Tomato plants exhibiting symptoms of Fusarium wilt were randomly collected at the beginning of summer 2022. From the necrotic tissue of tomato stems, different fungal species were isolated and purified in pure cultures. In this regard, tomato stems with vascular discoloration were carefully cut into short portions (3–5 cm long) and thoroughly cleaned with tap water. After being surface-disinfested in sodium hypochlorite (300 mg/L, 2%) for 2 min, tomato stem segments were given a thorough cleaning with sterile water. They were placed on a streptomycin sulfate-supplemented potato dextrose agar (PDA) plate after being dried on sterile filter paper. At a temperature of 26 °C, fungal cultures were incubated for two weeks. The cultivated fungal species were firstly morphologically identified using relevant identification keys [30,31]. DNA analysis was then used for molecular identification and phylogenetic confirmation.

2.3. Molecular Identification of Fusarium Strains

For fourteen days, one disc agar plug (5 mm) was cut from the tip of each of the three Fusarium species and cultured in its own tiny flask with 50 mL of sterilized potato dextrose broth (PDB) at 26 °C. *F. oxysporum* mycelium of each one was incubated at 26 °C for 6 days, then strained through cheesecloth, washed thoroughly with sterile water, and then put through sterilized filter paper to eliminate any remaining extra H_2O. A fine powder was finally produced by grinding approximately 100 mg of the collected fungal mycelium in the presence of liquid nitrogen. Following the instructions presented by the manufacturer of the DNeasy plant mini kit (Qiagen, Hilden, Germany), nucleic acid of each of the three Fusarium species was extracted from the ground fungal mycelium and separately deposited in a 1.5 mL micro-centrifuge tube. To confirm that all three *F. oxysporum* isolates belonged to the same species, we used the species-specific primer pair uni-F/uni-R [31]. The PCR experiments were carried out following [32]. PCR reactions were performed as described in our previous work [14], and after amplification, the PCR products were electrophoresed in agarose gel with 1%. The same forward and reverse primers were used to purify and sequence the PCR results. The BioEdit sequence alignment editor was used to analyze ABI trace files to generate contigs. At the end, the experimental sequence data of the three Fusarium isolates were deposited in GenBank.

2.4. CH@CuO NPs Synthesis and Characterization

Chitosan nanoparticles (CH NPs) were firstly prepared as indicated in [33]. The produced CH NPs were then purified and appropriately propagated using centrifugation and ultra-sonication multiple times. As the second phase in the synthesis process, chemical precipitation was used to produce copper oxide nanoparticles (CuO NPs), following a typical method described in prior research [34].

Only 0.5 g of the prepared CuO NPs was added to 50 mL of the newly formed chitosan (CH) NPs solution, and after sixty minutes of sonication, the mixture was combined into a

homogeneous suspension, and CH@CuO NPs were formed. The final product underwent continuous double-distilled water washing, 8000 rpm centrifugation, and vacuum oven drying. After that, the product was stored at 4 °C for subsequent analysis. Through use of a TECNAI 10 (TEM, Philips, Amsterdam, The Netherlands) transmission electron microscope, the nanocomposite was characterized. Samples were produced by dissolving 1 mg of CH, CuO, and CH@CuO NPs in 1 mL of deionized sterilized water, and then applying a single drop of the resulting solution to previously coated copper TEM grids that had been coated with carbon. The grids were subsequently dried at ambient temperature for 3–4 h, and the excess solution was eliminated with blotting paper. The Fourier-transform infrared spectroscopy (FTIR) measurement was carried out through the KBr pellet (FTIR grade) method in 1:100 ratio for 10 mg of each of the three formed nanoparticles powder and mixed with a pinch of potassium bromide (Himedia FTIR graded) in a crucible and was made into pellets by hydraulic press. The formed pellets were then analyzed using Fourier transform infrared (FTIR) spectrophotometry (Avatar-300, Nicolet, Green Bay, WI, USA). Using 16 average scans, the chemical functional groups that induced the CH NPs and CuO NPs to interact were identified at wavelengths between 400 and 4000 cm^{-1}.

2.5. In Vitro Antifungal Activity of CH@CuO NPs

By applying the agar dilution technique, the antifungal activity of the produced CH@CuO NPs with a particle size of 60 nm was assessed against three isolated *F. oxysporum* strains. Briefly, the agar medium was supplemented with produced CH@CuO nanoparticles at 3 different concentrations (1, 25, and 50 mg/L). From the margin of an 8-day-old fungal culture, a tiny disc of vigorous mycelial growth from each *F. oxysporum* strain (0.5 cm in diameter) was collected and plated in the middle of each PDA plate. After that, the fungal inoculation plates were then carefully incubated for about 8 days at 26 ± 2 °C. In order to evaluate the antifungal effect of CH@CuO NPs, the radial growth of *F. oxysporum* hyphae in each inoculation plate was measured, as shown in [32]:

$$\text{Inhibition (\%)} = [(T\_t)/T] \times 100 \quad (1)$$

where t represents the radial fungal growth of *F. oxysporum* hyphae on the PDA cultivated plate containing the three CH@CuO NP preparations, and T represents the radial growth of *F. oxysporum* hyphae on the control plate. As a positive control, the commercially available conventional fungicide Kocide 2000 (Certis, Columbia, MD, USA) was used. All in vitro laboratory experiments were applied three times under sterilized controlled conditions.

2.6. Imaging Using Fluorescence Microscopy

For the purpose of this experiment, fresh *F. oxysporum* conidial suspensions (50 mL, 3×10^7) were treated with an equal volume of CH@CuO NPs (at conc. 1 mg/L) and incubated at 26 ± 2 °C for one hour. The samples were subsequently stained for a period of twenty minutes with 10 mL of propidium iodide solution (PI; Sigma-Aldrich, Saint Louis, MO, USA; excitation/emission at 535 nm/617 nm). The slide counter was subsequently continuously dyed for 7 to 10 min in darkened light with a 10 mL solution containing 4′-6-diamidino-2-phenyl-indole (DAPI; Sigma-Aldrich, Saint Louis, MO, USA) [35]. Deionized water was used on the untreated samples as a control. The samples were then examined using an inverted fluorescent microscope (Nikon Eclipse Ti, Tokyo, Japan). The percentage of cell death (indicated in PI-stained cells, which represent dead fungal spores) was determined by dividing the number of PI-stained cells by the total number of DAPI- or PI-stained cells.

2.7. Preparation of Fusarium Inoculum

Initially, the pathogenic FOL isolates were cultured on a semi-strengthened PDA medium for about a week. The fungal inoculum was mixed properly in sorghum meal. In this regard, approximately 200–250 g of sorghum (*Sorghum bicolor* (L.) Moench)-cleaned seeds was immersed in H_2O in one-quart Mason jars overnight before being sterilized in au-

toclave two times. After allowing the sorghum seeds to cool in an autoclave, 8 mycelial plugs containing Fusarium conidial spores were carefully added to every jar. After 4 weeks, the sorghum with the grown fungal cultures was collected and dried in the air. The inoculum for the tomato root infection assay was prepared by combining 1 part Fusarium-infested sorghum with about 100 parts of a sterile 1:2 soil: sand mixture in sterilized plastic pots (10 cm diameter × 20 cm height).

2.8. In Vivo Antifungal Analysis of CH@CuO NPs

CH@CuO NPs were firstly dissolved in H_2O at two concentrations of 1 and 50 mg/L. Thirty-day-old tomato seedlings (cv. TH99806) were carefully transferred from their wetted soil and soaked in 50 mL CH@CuO NPs solution of each conc. (1 and 50 mg/L) separately for 30 min. For each NP concentration and control, nine plant replicates were set up. Seedlings were gently re-transplanted in the infected soil after incubation (4–5 seedlings per pot), and all treated plants were grown in a greenhouse. The positive and negative controls were seedlings challenged with the chemical fungicide "Kocide 2000" and mock-treated with H_2O, respectively. Startling on day ten post-inoculation (dpi), the number of tomato plants exhibiting symptoms of wilt symptoms was recorded for measuring the CH@CuO NPs' activity.

2.9. Analysis of Plant Height, Dry Weight, and Photosynthetic Pigments

Tomato plants' responses to (1, 25, and 50) mg/L concentrations of CH@CuO NPs were evaluated for changes in their dry weight, and also the photosynthetic pigments including (chlorophyll and the content of carotenoids). Dry weight and plant height were measured at 75 days after germination.

The levels of pigment were assessed by dissolving about 100 milligrams of plant tissue from each experimental group, including the untreated control, in 7 mL of dimethyl sulfoxide (DMSO). The solution was then heated to 65 °C until all chlorophylls and carotenoids were released into the resulting solution. The absorbance of the solution was measured using a Unico UV-2100 spectrophotometer (manufactured by Unico Instrument Co., Ltd., Shanghai, China) and was taken after incubation [36]. The absorbance was determined at 452, 644, and 663 nm using 95% ethanol as a blank. The chlorophyll and carotenoid contents were expressed as mg/g FW (fresh weight) [37].

2.10. Analysis of Peroxidase (POD) and Chitinase Activities

Following a method developed by [38] and modified by [39], peroxidase activity for each of the treated samples was monitored in comparison to the untreated ones. Similarly, [40] methodology was also used to quantify chitinase activity. In each sample, the supernatant absorbance was calculated [41,42].

2.11. Statistical Analyses

To validate the statistical variations among treatments, the acquired data were subjected to a one-way analysis of variance (ANOVA) and Duncan's multiple range test [43]. Using SPSS software version 8.0, means were compared using the Least Significant Difference (LSD) test at ($p < 0.05$). The results of each investigation were performed in triplicate, and they were presented as average standard deviation (SD). Graphs were also developed and edited using GraphPad Prism 9 software.

3. Results and Discussion

3.1. Morphological Characterization of the Fusarium Isolates

In order to examine the potential antifungal effect of chitosan-loaded copper oxide nanoparticles (CH@CuO NPs) against the pathogenic fungus *F. oxysporum*, we firstly isolated three wild strains of this fungus infecting tomato plants that were growing in Giza, Egypt, in 2022, and exhibited signs of wilting. The three isolated strains, named FOL1, FOL2, and FOL3, were firstly identified based on their morphological characteristics.

The fungal mycelia of all the FOL isolates were slightly white to slightly pink in color on PDA plates [43].

It was observed that all three fungal isolates produced individual microconidia, which had an ovate-to-slightly reniform shape and lacked septa. Moreover, the size of the microconidia ranged from 7.22 to 15.09 µm in length and 2.23 to 4.1 µm in width. Furthermore, the produced macroconidia of the three isolates displayed an elliptical shape with gradually pointed ends and possessed three transverse septa. Additionally, the average size of the produced macroconidia varied between 27.2 and 45.6 µm in length and 2.9 and 4.3 µm in width [43,44].

3.2. Molecular Identification of the Isolated FOL Strains

The identification of the three Fusarium isolates as *F. oxysporum* was validated by employing the use of the polymerase chain reaction (PCR) technique. The PCR studies were conducted using the uni-F/uni-R primer pair, resulting in the generation of DNA products with an average size of approximately 670 base pairs. PCR amplification was performed using the primers that had been previously used, confirming that the isolated strains are indeed identified as *Fusarium oxysporum f.* sp. *Lycopersici* (FOL) [35,45]. The BLASTn analysis conducted on the amplification products of FOL1, FOL2, and FOL3 sequences revealed e-values of zero and similarities of 98.95% with GenBank *F. oxysporum* accessions no. LC089734.1. This outcome provides strong support for the phenotypic characterization of all three Fusarium isolates. The ITS regions of *F. oxysporum* FOL1, FOL2, and FOL3 isolates were submitted to GenBank and assigned accession numbers OR354466, OR354916, and OR354917, respectively.

3.3. Synthesis and Characterization of CH@CuO NPs

The TEM results indicated the formation of CH NPs with a semi-transparent network shape (Figure 1A), with a 25 nm particle size. While CuO NPs are spherically shaped with a (19 nm) particle size (Figure 1B). In Figure 1C, CH@CuO NPs exhibited an irregular shape with 54.22 nm in size, displaying several dark spots that are securely immobilized on the surfaces of CH nanoparticles. (Figure 1C). Additionally, the noticeable aggregated structures in Figure 1 were also in agreement with data obtained by [46], which may be explained by the catalytic activity of the CuO NPs surface [47], and which can illustrate further the higher antifungal activity of CH@CuO NPs [48].

On the other hand, the Dynamic light scattering (DLS) analysis revealed that the particle sizes of the synthesized CH NPs, CuO NPs, and CH@CuO NPs were approximately 30.36 $\pm$ 1.2 nm, 24.01 $\pm$ 2.4 nm, and 60.0 nm $\pm$ 1.4 nm, respectively. (Figure 1D–F). The relative increment in the particle size of CH NPs, CuO NPs, and CH@CuO NPs in the case of DLS measurements in comparison to those of TEM results may be because of the influence of Brownian motion in the solution [49]. According to the FTIR findings, the FTIR spectrum of CH NPs exhibited several peaks that corresponded to various functional groups. These included the stretching vibration peaks of O-H (3421 cm^{-1}), C=C (1650 cm^{-1}), and C-O (1290 cm^{-1}), as well as the asymmetric stretching vibration of C-H bonds in -CH3 and -CH2 (2930 cm^{-1}) and the in-plane bending vibration of C-H (1423 cm^{-1}), which was noticeably reduced after loading CuO NPs on CH NPs surfaces, as indicated (Figure 2). Although there was no noticeable disappearance in the functional groups of CH NPs after loading with CuO NPs and generating CH@CuO NPs, there was a significant reduction in the transmittance (%) of bands after loading with CuO NPs, particularly O-H, C=C, and C-H. Taken together, these results indicate that CuO NPs were successfully immobilized on the surface of the CH NPs.

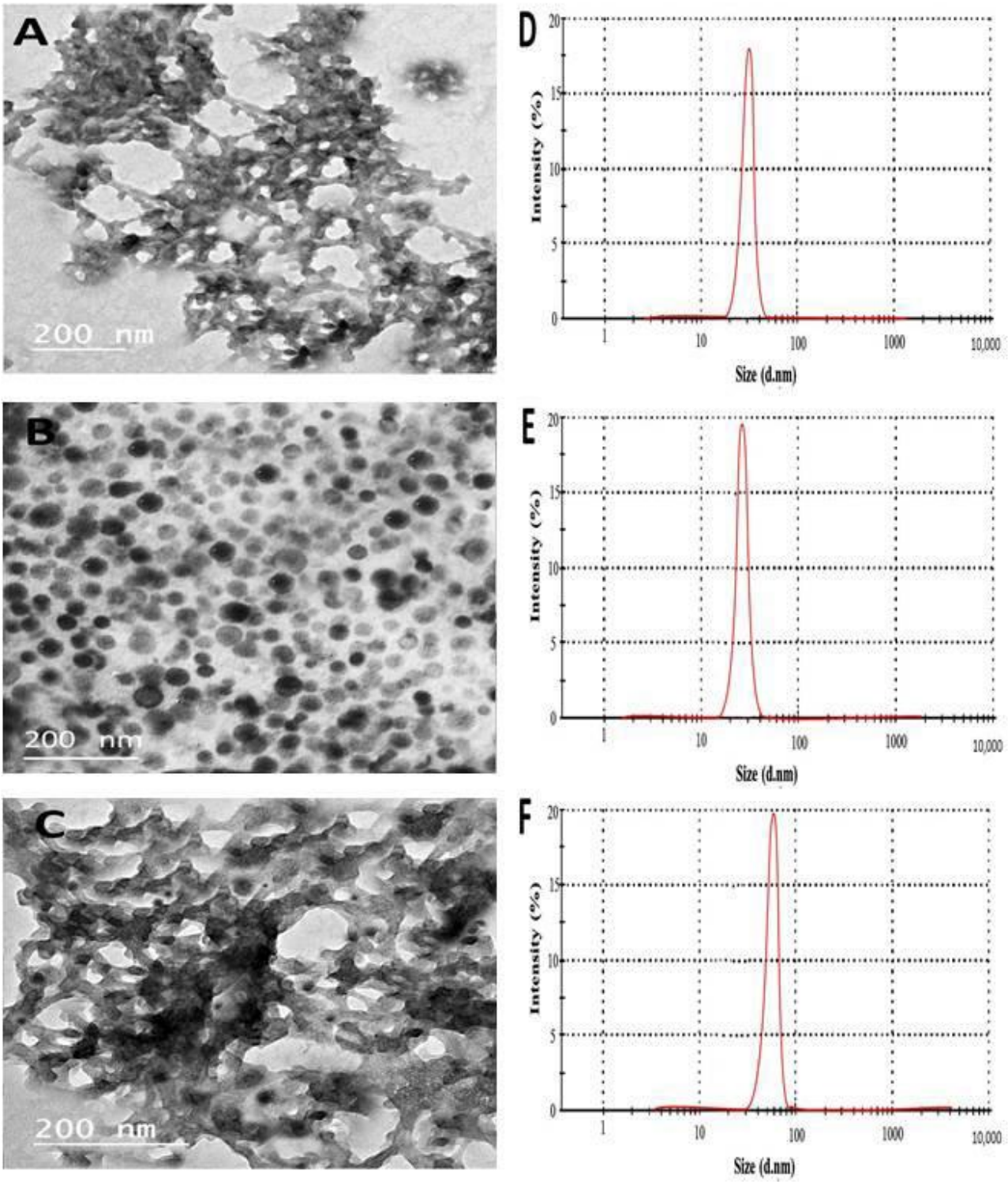

Figure 1. Transmission electron microscope (TEM) images of CH NPs (**A**), CuO NPs (**B**), CH@CuO NPs (**C**), and their DLS measurements (**D**–**F**) respectively.

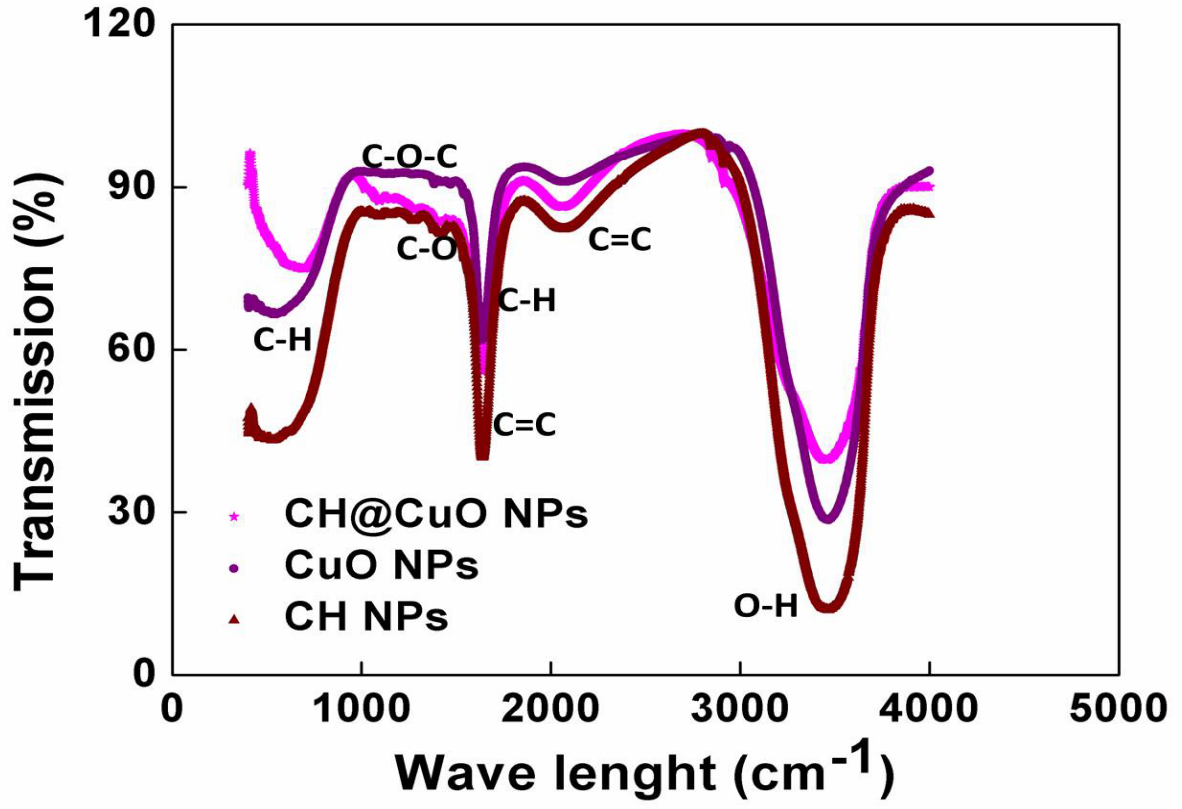

Figure 2. The FTIR spectra of the formed CH@CuO NPs, CuO NPs, and CH NPs (as indicated), showing different peaks representing functional groups.

3.4. Antifungal Effect of the Produced CH@CuO NPs

The antifungal effect of the produced CH@CuO NPs with 60 nm particle size was next investigated in vitro against the three isolated *F. oxysporum* strains at three different doses (1, 25, and 50 mg/L). The antifungal activity of the nanocomposite increased as the concentration of CH@CuO NPs increased (Table 1). The observed result can be attributed to the increased surface area of CH@CuO NPs with higher concentrations compared to their larger counterparts. This greater surface area facilitates enhanced interactions with fungal cell structures, thus explaining the finding and more rapid Cu ion release [50,51]. Remarkably, while analyzing the antifungal impact of CH@CuO NPs concentrations at varied concentrations, the statistical analysis suggested that NPs concentration is a major factor. Table 1 illustrates the inhibition of mycelial growth for FOL1, FOL2, and FOL3 following various treatments utilizing those produced CH@CuO NPs.

The acquired outcomes showed that the three tested *F. oxysporum* isolates had the highest percentage (%) of fungal growth inhibition rate at 50 mg/L, with significant values of 96.48 ± 0.32, 95.27 ± 0.12, and 91.15 ± 1.2% for FOL1, FOL2 and FOL3, respectively, comparing to a control treatment with the fungicide (77.34 ± 0.33, 77.12 ± 0.33, and 80.5 ± 1.2%, respectively), after 8 days of incubation (Table 1). In summary, these compelling findings provide support for the potential of CH@CuO NPs as a viable alternative to traditional chemical fungicides in protecting plant crops. This aligns with previous research studies that have demonstrated the diverse mechanisms through which both CH and CuO NPs can effectively inhibit microbial pathogens [52], allowing them to be used as an alternative to conventional synthetic pesticides for controlling a variety of microbial pathogens infecting plants. This will greatly lessen the harmful impacts of toxic chemical fungicides, particularly on edible crops and vegetables [53,54].

Table 1. The average percent growth inhibition with statistical difference caused by CH@CuO NPs "at 60 nm size" with three different concentrations against three pathogenic *F. oxysporum* isolates.

Pathogen	Treatment		Concentration	Inhibition Rate (%)		
				4 Days	6 Days	8 Days
F. oxysporum (FOL1)	CH@CuO nanocomposite		1 mg/L	92.15 ± 1.56 [a]	93.22 ± 1.2 [a]	96.22 ± 1.35 [a]
			25 mg/L	94.0 ± 2.4 [b]	95.0 ± 0.33 [b]	96.32 ± 0.33 [a]
			50 mg/L	95.10 ± 1.24 [c]	95.10 ± 1.22 [b]	96.90 ± 1.0 [b]
	Controls	CH NPs	1 g/L	5.55 ± 0.0 [f]	9.45 ± 1.2 [e]	11.11 ± 0.0 [e]
		CuO NPs	1 g/L	19.22 ± 0.0 [e]	35.12 ± 0.46 [d]	33.33 ± 1.1 [d]
		Kocide 2000	2.5 g/L	65.3 ± 0.1 [d]	67.2 ± 0.22 [c]	77.34 ± 0.33 [c]
F. oxysporum (FOL2)	CH@CuO nanocomposite		1 mg/L	90.06 ± 0.22 [a]	92.35 ± 0.10 [a]	94.22 ± 1.2 [a]
			25 mg/L	92.06 ± 0.33 [a]	93.36 ± 0.25 [b]	95.80 ± 0.2 [b]
			50 mg/L	93.08 ± 0.45 [b]	94.55 ± 0.22 [c]	95.80 ± 1.43 [b]
	Controls	CH NPs	1 g/L	2.27 ± 0.3 [e]	7.89 ± 1.4 [f]	8.33 ± 0.20 [e]
		CuO NPs	1 g/L	25.00 ± 0.46 [d]	33.33 ± 0.44 [e]	38.88 ± 1.1 [d]
		Kocide 2000	2.5 g/L	64.5 ± 0.5 [c]	69.2 ± 0.45 [d]	77.12 ± 0.33 [c]
F. oxysporum (FOL3)	CH@CuO nanocomposite		1 mg/L	86.95 ± 3.5 [a]	88.24 ± 2.33 [a]	91.0 ± 3.4 [b]
			25 mg/L	88.13 ± 2.2 [b]	89.07 ± 1.2 [a]	90.22 ± 1.5 [a]
			50 mg/L	90.72 ± 1.4 [c]	88.77 ± 0.7 [a]	92.24 ± 1.4 [c]
	Controls	CH NPs	1 g/L	8.22 ± 0.33 [f]	10.33 ± 1.2 [d]	12.11 ± 0.0 [f]
		CuO NPs	1 g/L	20.22 ± 1.7 [e]	30.12 ± 0.0 [c]	33.44 ± 0.0 [e]
		Kocide 2000	2.5 g/L	70.3 ± 0.4 [d]	75.2 ± 0.33 [b]	80.5 ± 1.2 [d]

Mean values with different labels ([a, b, c, d, e, f]) were significantly different ($p < 0.05$) according to one-way ANOVA followed by Duncan's multiple range test. Data are shown as mean ± SD. SD: Standard Deviation of three repeats per treatment.

3.5. FOL Cell Viability after Treatment with CH@CuO NPs

Under a fluorescence microscope, PI and DAPI were used to examine CH@CuO NPs' antifungal activity against one of the three tested *F. oxysporum* isolates (FOL1 was selected). The PI dye is unable to pass through cell membranes and selectively labels damaged cells by emitting red fluorescence, whereas DAPI can enter intact living cells and firmly attach to nucleic acids, emitting blue fluorescence [55,56]. In this regard, 1 mg/L of CH@CuO NPs (60 nm in size) was added to a culture of the FOL1 isolate. Through a fluorescence microscope, DAPI- and PI-stained spores were examined from the treated fungal culture. The culture treated with CH@CuO nanoparticles exhibited a predominance of red propidium iodide (PI) fluorescence, which is indicative of cellular death (Figure 3B), in contrast to the untreated control culture, which showed only blue fluorescence (Figure 3A).

3.6. CH@NPs Activity of CH@CuO NPs against Fusarium Wilt Disease

Further investigation was conducted to evaluate the in vivo antifungal activity of CH@CuO nanoparticles, with the goal of controlling Fusarium wilt disease in tomato plants. Disease severity was assessed in tomato plants treated with 1, 25, or 50 mg/L of CH@CuO NPs for 75 days (Figure 4). Plants treated with a conventional fungicide were also included in the experiment. Disease symptoms were clearly visible in mock-treated tomato plants as early as 12 dpi, but disease symptoms were minor and mostly delayed in tomato-treated plants. A traditional fungicide (Kocide 2000) control treatment of tomato plants delayed and decreased disease symptoms, but to a smaller extent than CH@CuO NPs. Figure 4B displays images of mock-treated, 1, 25, or 50 mg/L CH@CuO NP-treated, or Kocide-treated tomato plants transplanted into infected soil. At 75 dpi, tomatoes treated with 1, 25, or 50 mg/L of CH@CuO NPs exhibited healthier status than mock-treated or

Kocide-treated plants (Figure 4B). Most importantly, plants exposed to 25 or 50 mg/L of CH@CuO NPs showed no significant changes (Figure 4B).

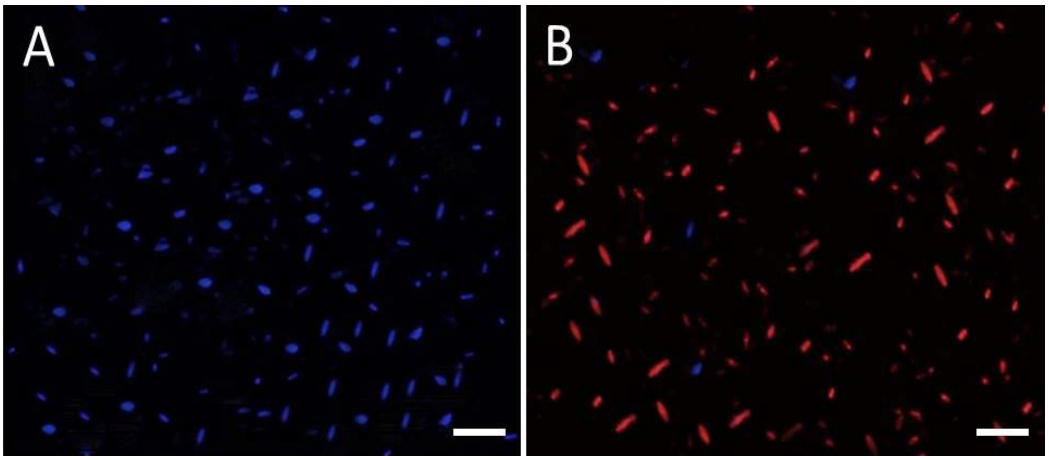

Figure 3. Fluorescence microscopy analysis of fungal cell viability: FOL fungal spores (**A**) non-treated or (**B**) treated with CH@CuO NPs were stained with DAPI (stains live spores in blue) and PI (stains dead spores in red) and visualized, (bars = 40 μm).

Importantly, tomato plants that were soaked in CH@CuO NPs solution for 30 min prior to being transplanted into infectious soil showed a remarkably high reduction in the disease severity of wilt in tomatoes treated with 25 and 50 mg/L CH@CuO NPs, respectively, disease severity was decreased by 96.0 and 98% compared to that in cases where a chemical fungicide was applied (90%) or CH@CuO NPs at 1 mg/L showing 91.5% reduction in disease severity (Figure 4A). Importantly, neither 1 mg/L nor 50 mg/L of CH@CuO NPs produced any obvious phytotoxicity. These findings suggested that CH@CuO NPs, even at a relatively low concentration of 1 mg/L, outperform the chemical fungicide Kocide in terms of antifungal activity. According to previous research [57], when cultivated in soil infested with the pathogenic fungi "*Verticillium dahliae* and *Fusarium oxysporum f*. sp. *lycopersici* (FOL)", tomato and eggplant development was promoted by CuO NPs to a greater extent than by any of the other six metallic oxide nanoparticles (TiO, ZnO, MnO, AlO, NiO, or FeO).

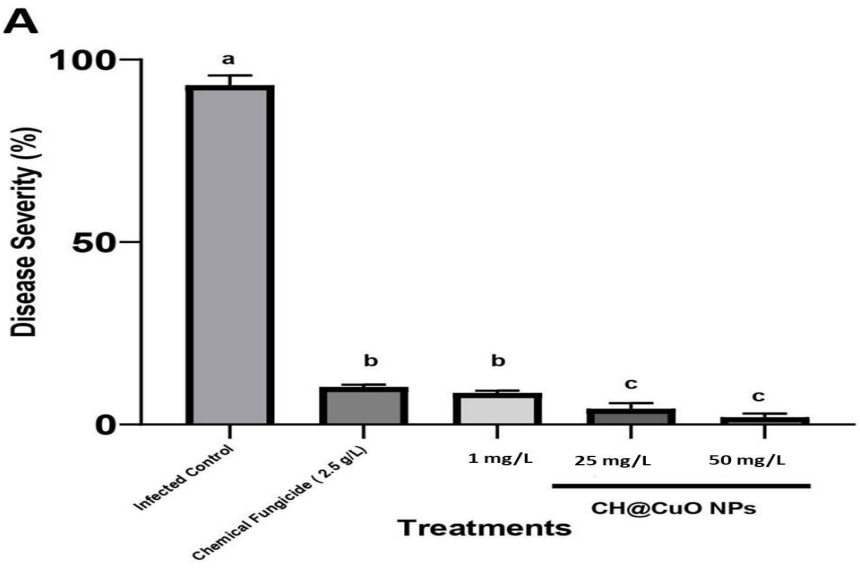

Figure 4. *Cont.*

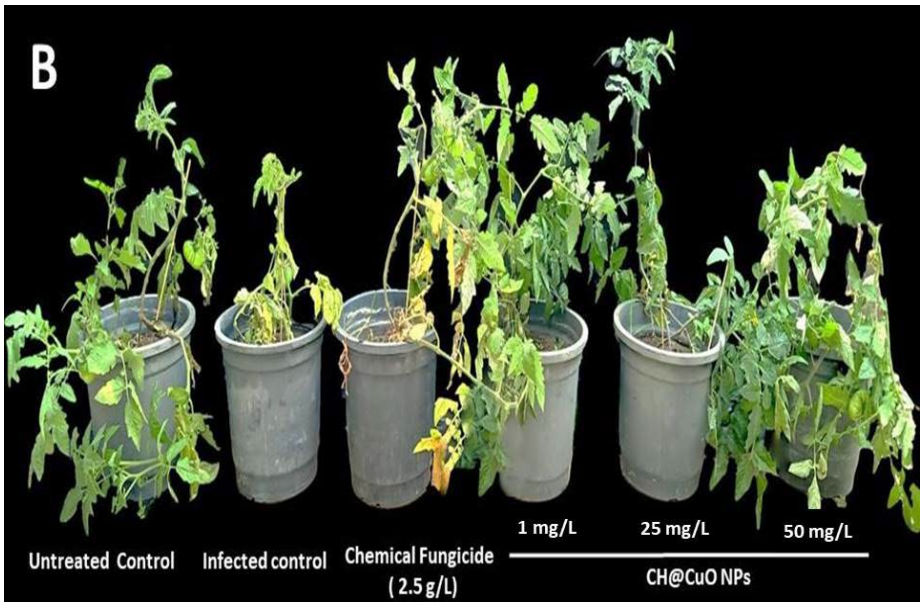

Figure 4. (**A**) Disease severity index in percentage (%) of tomato plants non-treated infected tomato plants (infected control), treated with CH@CuO NPs at (1, 25, and 50 mg/L) or the conventional chemical fungicide Kocide 2000 and, then, challenged with FOL1 isolate. Average and standard errors of nine replicates are shown. Bars with the same letters are not statistically significant based on the LSD test ($p < 0.05$). (**B**) In vivo treatments of tomato plants with CH@CuO nanoparticles at (1, 25, and 50 mg/L) concentrations in comparison to tomato plants treated with the commercial fungicide (Kocide 2000 "2.5 g/L") after being challenged with FOL1 isolate. Untreated non-infected tomato plants (Untreated Control) and Untreated infected control tomato plants showing Fusarium wilt symptoms (Infected control) were used as controls. Pictures were taken at 75 dpi.

Regarding this, numerous studies have even suggested that Chitosan has a wide variety of antifungal actions on pathogenic fungi in plants [58]. Additionally, according to certain studies, CH was beneficial to tomato seed germination and seedling growth [59]. Our results, however, significantly demonstrate that season-long pathogen suppression and yield improvement were achieved with just one application of CuO NPs delivered on CH@CuO NPs at a very low concentration (1 mg/L). At the beginning of the growing season, premature seedling plants might become infected with Fusarium wilt [60,61], emphasizing the significance of a disease/treatment window. This could be one explanation for the long-lasting advantages of CH@CuO NPs. The host's defense may drastically reduce or suppress Fusarium infection and also delay the onset of Fusarium wilt disease symptoms if there are enough CH@CuO NPs in plant root cells, preventing the disease from severely spreading. Another potential mechanism is that CH@CuO NPs stimulate host-defense-related gene expression. To deal with Fusarium infection, tomato plants would benefit from this. Although our results are promising, they do not provide a detailed explanation of the precise mechanism by which CH@CuO NPs inhibit fungal growth. According to a prior theory [62], CH@CuO NPs can translocate into other plant tissues and pass through root cells, causing systemic resistance. Moreover, other reports have suggested that the unique control release matrix of chitosan molecules can generate active components with better results in plant disease management whose concentration has been established and their release has been sustained for a while. Improved bioavailability, mobility, and long-term accumulation of bioactive substances encapsulated or loaded on chitosan's surface due to persistent release behavior is carefully regulated [63]. Moreover, with the known role of CuO as an antimicrobial, other studies have reported that oligo-chitosan treatment is responsible for the increment of phenolic compounds such as anthocyanins, which are responsible for protection against biotic factors [64].

On the other hand, the excellent antimicrobial efficacy of copper-based compounds, particularly copper oxide (CuO), has been observed against a wide spectrum of microbes [65–68]. In addition, copper is a necessary plant micronutrient that aids in plant growth and disease resistance. More interestingly, copper is required for the creation of key plant defense proteins, such as plastocyanin, peroxidase, and copper multiple oxidases, in response to pathogen infections [69]. These nonspecific immune responses to infection can protect against a wide range of diseases.

3.7. Potential Effect of CH@CuO NPs on Flowering and Photosynthetic Pigments

The results indicate that the treatment of tomatoes with CH@CuO NPs enhanced or stimulated their early flowering, which significantly affected an increase in tomato production. In this regard, all treatments resulted in an apparent rise in the quantity of flowers (Figure 5C). When compared to the chemical fungicide treatment, the NPs application at concentrations (1, 25, and 50 mg/L) significantly encouraged tomatoes' early flowering as their concentration increased (Figure 5C). When compared to plants treated with conventional fungicides, all plants treated with NPs showed an apparent rise in plant height and dry weight (Figure 5B). In conclusion, plants with their roots submerged in the NPs solution exhibited a considerable beneficial behavior. These findings are consistent with data reported in [53]. The interesting results included the finding that all NP treatments significantly enhanced photosynthetic pigments in comparison to treatments with traditional chemical fungicides (Figure 5A). According to previous findings, which indicated a dose-dependent loss in fresh weight, root length, and the total content of chlorophyll [55], these findings demonstrate that the 60 nm CH@CuO NPs considerably raise the level or quantity of photosynthetic pigments in the treated plants. However, in that investigation, bigger (30 nm) free CuO NPs were employed. Together, these findings show that copper oxide loaded on Chitosan nanoparticles has two different functional purposes in both improving plant development and generating a defense response to protect the treated plants against diseases including Fusarium wilt. These results might be explained by the distinctive physicochemical characteristics of these NPs, such as their stability, small size, and water solubility, which provide them with the potential to penetrate the plant system more easily than other important nutrients.

3.8. Influences of CH@CuO NPs Treatments on Some Defense Enzyme Activity in Treated Tomato Plants

Two defense-related enzymes were investigated to learn more about the interaction of *F. oxysporum* with tomato after dipping in CH@CuO NPs. The results demonstrated that FOL inoculation increased the activity of the two defense-related enzymes studied in the three CH@CuO NPs treatments relative to the un-inoculated control plants. The infected plants had higher peroxidase and chitinase activity than the untreated plants in the pot experiment. However, it was discovered that a gradual increase in CH@CuO NPs concentrations in root treatments dramatically improved both peroxidase and chitinase activity as compared to the infected control. Thus, the CH@CuO NPs treatment stimulated these enzymes' activity over the pathogen effect. CH@CuO NPs at 50 mg/L provided the highest increase in both peroxidase and chitinase activity (Figure 6), followed by its concentration at 25 mg/L. Simultaneously, Kocide 2000 (2.5 g/L) increased both peroxidase and chitinase activity. Those findings imply that when CH@CuO NPs are applied exogenously, tomato becomes more resistant to FOL infections. This is in line with previous research that demonstrates how exogenously applied generated compounds can cause their hosts to develop resistance by increasing the quantities of host defense enzymes and pathogen-related (PR) proteins. It also suggests that the CH@CuO NPs promote systemic resistance in the host plants, making them less susceptible to infection [70].

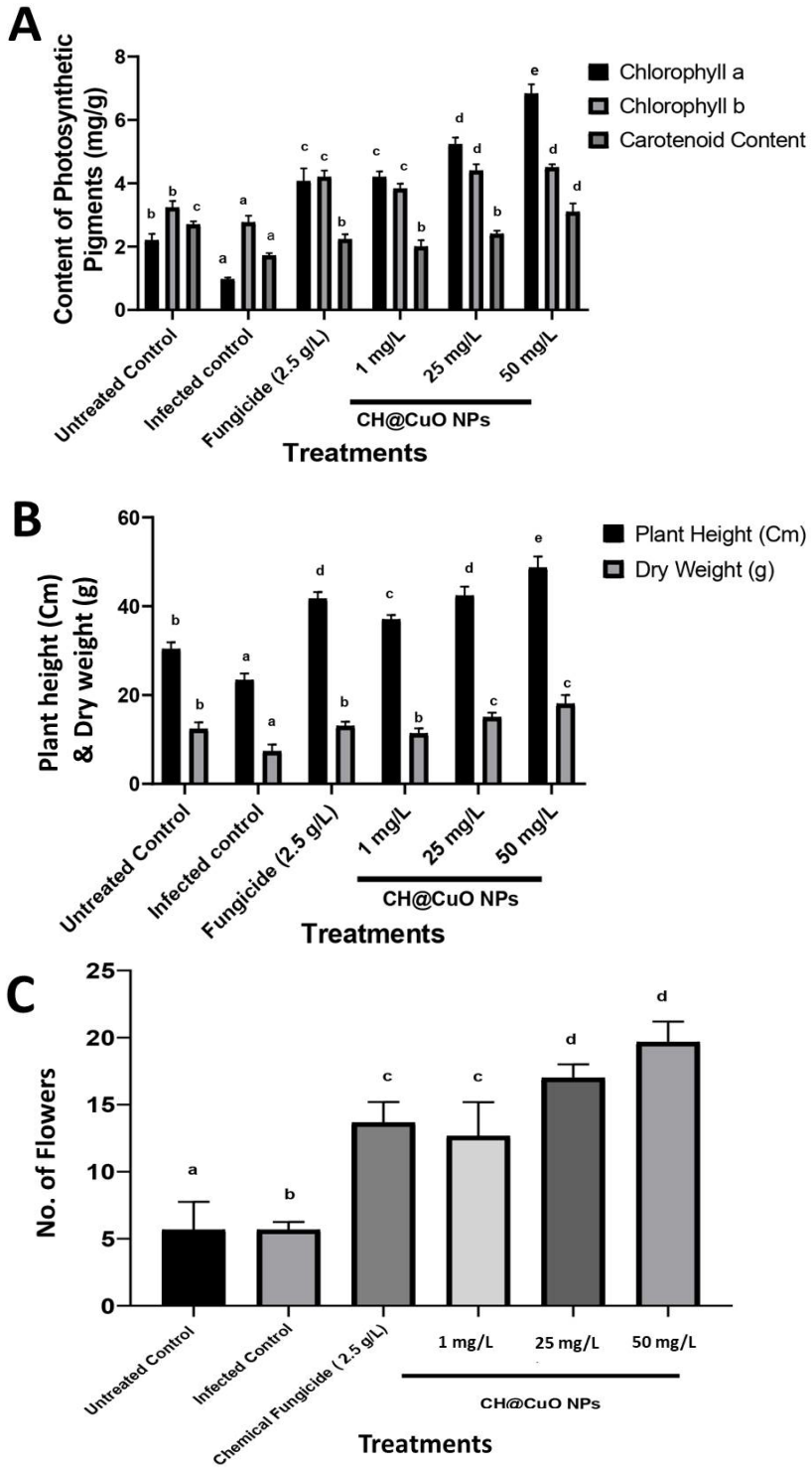

Figure 5. Effect of CH@CuO NP treatments at (1, 25, and 50 mg/L) concentrations on some physiological parameters of tomato-treated plants: (**A**) photosynthetic pigments (Chlorophyll a, b, and carotenoids); (**B**) Plant height and Dry weight; and (**C**) Flower increment. In comparison with tomato plants treated with the commercial fungicide (Kocide 2000 "2.5 g/L") after being challenged with *F. oxysporum* (FOL1 isolate). Untreated non-infected tomato plants (Untreated Control) and Untreated infected control tomato plants showing Fusarium wilt symptoms (Infected control) were used as controls. The small letters on the bars denote statistically significant differences ($p < 0.05$) among the averages of the corresponding control and nanocomposite at the same concentrations.

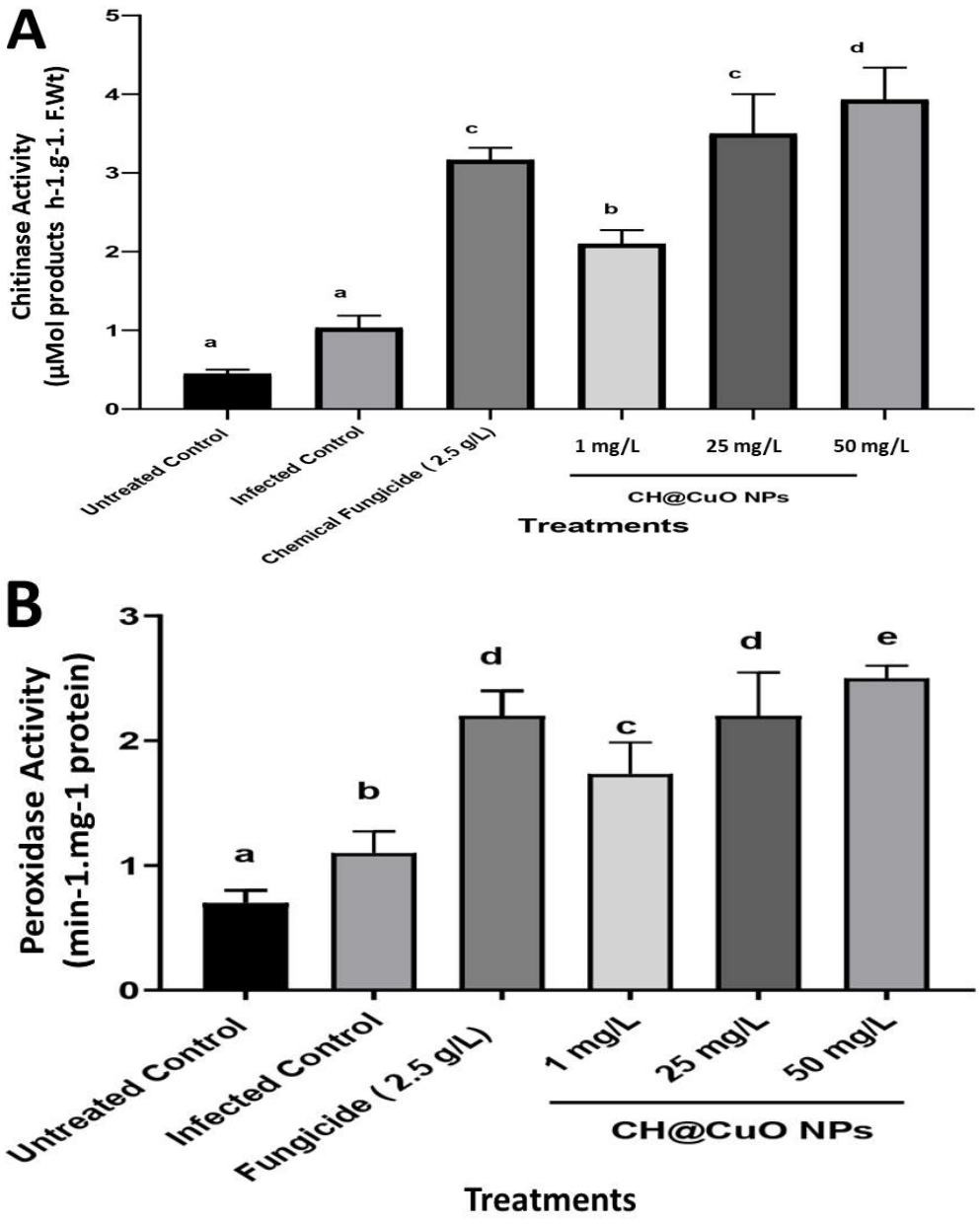

Figure 6. Effect of CH@CuO NP treatments at (1, 25, and 50 mg/L) concentrations on some enzymatic activity of tomato-treated plants: (**A**) chitinase and (**B**) peroxidase enzymes. In comparison to tomato plants treated with the commercial fungicide (Kocide 2000 "2.5 g/L") after being challenged with *F. oxysporum* (FOL1 isolate). Untreated non-infected tomato plants (Untreated Control) and Untreated infected control tomato plants showing Fusarium wilt symptoms (Infected control) were used as controls. The small letters on the bars denote statistically significant differences ($p < 0.05$) among the averages of the corresponding control and nanocomposite at the same concentrations.

The increased activity and expression of PR proteins like chitinases, peroxidases, −1, 3-glucanases, and acid invertases correlate with the onset of induced systemic resistance in plants [71–73]. According to many studies, plant-derived compounds can help many crops grow more plants and reduce disease [74,75]. When dormant plant defense genes in healthy, uninoculated plants are activated by a range of situations, they can result in systemic resistance to disease. Increasing chitinase, protease, peroxidase, and AI enzyme activity, and also the expression of the genes for −1, 3-glucanase, and chitinase, has been shown to be effective against a number of fungal infections [74–78]. CH@CuO NP treatments at various doses provided defense in tomato plants against Fusarium infection

by increasing the levels of defense-related enzymes and pathogenesis-related proteins. These proteins may play an important role in reinforcing the host plant's cell walls in order to withstand FOL invasion. Because CH@CuO NPs are composed of carbon, it has been postulated that they may increase protein production in response to pathogen inoculation to activate their defense mechanisms and prevent pathogen entry or spread [78].

4. Conclusions

The purpose of this investigation was to determine or evaluate the potential effect of the produced CH@CuO NPs against three examined *F. oxysporum* isolates that infect cultivated tomato plants. First, spectroscopic and microscopic studies were functionalized in order to produce and also characterize CH@CuO NPs showing a 54.22 nm particle size, as indicated by TEM results. Then, in vitro growth investigations using the three fungal isolates were used to establish the nanocomposite's antifungal potential and the highest percentage (%) of fungal growth inhibition rate at 50 mg/L, with significant values of 96.48 ± 0.32, 95.27 ± 0.12, and 91.15 ± 1.2% for FOL1, FOL2, and FOL3, respectively, in contrast to a control treatment with the chemical fungicide (77.34 ± 0.33, 77.12 ± 0.33, and 80.5 ± 1.2%, respectively), after 8 days of incubation. Fluorescence analysis verified CH@CuO NPs' ability to control the fungal spores. Importantly, CH@CuO NPs demonstrated higher antifungal activity against the causal agent of the Fusarium wilt disease, reduced the disease severity by 91.5% at only 1 mg/L, and had substantial impact for up to 75 days in greenhouse experiments. In contrast, 2.5 g/L of Kocide 2000 is required to reduce disease in tomato plants by about 90%. Copper oxide is a plant nutrient, so it is noteworthy that research on copper oxide-treated plants revealed positive effects on flowering, plant height, dry weight, and defense enzymatic activity, as well as a buildup of photosynthetic pigments. Finally, the morphology of tissues from treated plants showed no evidence of phytotoxicity. Finally, we suggest that the produced CH@CuO NPs may be a promising nanocomposite product for crop protection against fungal diseases, which, interestingly, has positive side effects on plant growth and exhibits a significant antifungal action against *Fusarium oxysporum*.

Author Contributions: The study's design was motivated by all of the authors. M.A.M. developed the nanomaterials, while S.E.E.-A. carried out the characterization experiments. The in vitro and in vivo investigations were performed by M.A.M. and both M.A.M. and S.E.E.-A. acquired molecular fungal identification and sequencing analysis. M.A.M. completed writing the manuscript. All authors have read and agreed to the published version of the manuscript.

Funding: This research received no external funding.

Institutional Review Board Statement: Not applicable.

Informed Consent Statement: Not applicable.

Data Availability Statement: Not applicable.

Conflicts of Interest: The authors declare no conflict of interest.

References

1. Heuvelink, E.; Dorais, M. Crop Growth and Yield. *Crop Prod. Sci. Hortic.* **2005**, *13*, 85.
2. El-Ganainy, S.M.; Mosa, M.A.; Ismail, A.M.; Khalil, A.E. Lignin-Loaded Carbon Nanoparticles as a Promising Control Agent against *Fusarium verticillioides* in Maize: Physiological and Biochemical Analyses. *Polymers* **2023**, *15*, 1193. [CrossRef]
3. Dita, M.; Barquero, M.; Heck, D.; Mizubuti, E.S.; Staver, C.P. Fusarium wilt of banana: Current knowledge on epidemiology and research needs toward sustainable disease management. *Front. Plant Sci.* **2018**, *9*, 1468. [CrossRef]
4. Naguib, D.M. Control of Fusarium wilt in wheat seedlings by grain priming with defensin-like protein. *Egypt. J. Biol. Pest. Control* **2018**, *28*, 68. [CrossRef]
5. Shishido, M.; Miwa, C.; Usami, T.; Amemiya, Y.; Johnson, K.B. Biological control efficiency of Fusarium wilt of tomato by nonpathogenic *Fusarium oxysporum* Fo-B2 in di_erent environments. *Phytopathology* **2005**, *95*, 1072–1080. [CrossRef] [PubMed]
6. Gordon, T.R.; Martyn, R.D. The evolutionary biology of *Fusarium oxysporum*. *Annu. Rev. Phytopathol.* **1997**, *35*, 111–128. [CrossRef]

7. Selim, M.E.; Khalifa, E.Z.; Amer, G.A.; Ely-Kafrawy, A.A.; El-Gammal, N.A. Evaluation and characterization of some Egyptian *Fusarium oxysporum* isolates for their virulence on tomato and PCR detection of (SIX) effector genes. *J. Bioprocess. Biotechnol.* **2015**, *5*, 204.
8. Buonaurio, R.; Moretti, C.; Bertona, A.; Scarponi, L. Investigations on the Systemic Acquired Resistance Induced by Acibenzolar-S-Methyl in Tomato Plants Against *Pseudomonas syringae* pv. tomato. In *Pseudomonas Syringae and Related Pathogens*; Springer: Dordrecht, The Netherlands, 2003; pp. 475–482.
9. Ismail, A.M. Efficacy of Copper Oxide and Magnesium Oxide Nanoparticles on Controlling Black Scurf Disease on Potato. *Egypt. J. Phytopathol.* **2021**, *49*, 116–130. [CrossRef]
10. Dimkpa, C.O.; McLean, J.E.; Britt, D.W.; Anderson, A.J. Antifungal activity of ZnO nanoparticles and their interactive e_ect with a biocontrol bacterium on growth antagonism of the plant pathogen *Fusarium graminearum*. *Biometals* **2013**, *26*, 913–924. [CrossRef]
11. Krishna, V.; Pumprueg, S.; Lee, S.-H.; Zhao, J.; Sigmund, W.; Koopman, B.; Moudgil, B.M. Photocatalytic Disinfection with Titanium Dioxide Coated Multi-Wall Carbon Nanotubes. *Process Saf. Environ. Prot.* **2005**, *83*, 393–397. [CrossRef]
12. El-Gazzar, N.; Ismail, A.M. The Potential Use of Titanium, Silver and Selenium Nanoparticles in Controlling Leaf Blight of Tomato Caused by *Alternaria alternata*. *Biocatal. Agric. Biotechnol.* **2020**, *27*, 101708. [CrossRef]
13. Cordero, T.; Mohamed, M.A.; Lopez-Moya, J.-J.; Daròs, J.-A. A Recombinant Potato Virus y Infectious Clone Tagged with the Rosea1 Visual Marker (Pvy-Ros1) Facilitates the Analysis of Viral Infectivity and Allows the Production of Large Amounts of Anthocyanins in Plants. *Front. Microbiol.* **2017**, *8*, 611. [CrossRef] [PubMed]
14. Mosa, M.A.; Youssef, K. Topical Delivery of Host Induced RNAi Silencing by Layered Double Hydroxide Nanosheets: An Efficient Tool to Decipher Pathogenicity Gene Function of Fusarium Crown and Root Rot in Tomato. *Physiol. Mol. Plant Pathol.* **2021**, *115*, 101684. [CrossRef]
15. Mosa, M.A.; El-Abeid, S.E.; Khalifa, M.M.A.; Elsharouny, T.H.; El-Baz, S.M.; Ahmed, A.Y. Smart PH Responsive System Based on Hybrid Mesoporous Silica Nanoparticles for Delivery of Fungicide to Control Fusarium Crown and Root Rot in Tomato. *J. Plant Pathol.* **2022**, *104*, 979–992. [CrossRef]
16. Youssef, K.; de Oliveira, A.G.; Tischer, C.A.; Hussain, I.; Roberto, S.R. Synergistic Effect of a Novel Chitosan/Silica Nanocomposites-Based Formulation against Gray Mold of Table Grapes and Its Possible Mode of Action. *Int. J. Biol. Macromol.* **2019**, *141*, 247–258. [CrossRef]
17. Ismail, A.M.; Mosa, M.A.; El-Ganainy, S.M. Chitosan-Decorated Copper Oxide Nanocomposite: Investigation of Its Antifungal Activity against Tomato Gray Mold Caused by *Botrytis cinerea*. *Polymers* **2023**, *15*, 1099. [CrossRef]
18. Pradhan, S.; Patra, P.; Mitra, S.; Dey, K.K.; Jain, S.; Sarkar, S.; Roy, S.; Palit, P.; Goswami, A. Manganese Nanoparticles: Impact on Non-Nodulated Plant as a Potent Enhancer in Nitrogen Metabolism and Toxicity Study Both in vivo and in vitro. *J. Agric. Food Chem.* **2014**, *62*, 8777–8785. [CrossRef]
19. Choudhary, R.C.; Kumaraswamy, R.V.; Kumari, S.; Sharma, S.S.; Pal, A.; Raliya, R.; Biswas, P.; Saharan, V. Cu-Chitosan Nanoparticle Boost Defense Responses and Plant Growth in Maize (*Zea mays* L.). *Sci. Rep.* **2017**, *7*, 9754. [CrossRef]
20. Karlsson, K.R.; Cowley, S.; Martinez, F.O.; Shaw, M.; Minger, S.L.; James, W. Homogeneous Monocytes and Macrophages from Human Embryonic Stem Cells Following Co-culture-Free Differentiation in M-CSF and IL-3. *Exp. Hematol.* **2008**, *36*, 1167–1175. [CrossRef]
21. Rubina, M.S.; Vasil'kov, A.Y.; Naumkin, A.V.; Shtykova, E.V.; Abramchuk, S.S.; Alghuthaymi, M.A.; Abd-Elsalam, K.A. Synthesis and Characterization of Chitosan–Copper Nanocomposites and Their Fungicidal Activity against Two Sclerotia-Forming Plant Pathogenic Fungi. *J. Nanostruct. Chem.* **2017**, *7*, 249–258. [CrossRef]
22. Xu, J.; Zhao, X.; Han, X.; Du, Y. Antifungal Activity of Oligochitosan against *Phytophthora capsici* and Other Plant Pathogenic Fungi in vitro. *Pestic. Biochem. Physiol.* **2007**, *87*, 220–228. [CrossRef]
23. Muzzarelli, R.A.A.; Muzzarelli, C.; Tarsi, R.; Miliani, M.; Gabbanelli, F.; Cartolari, M. Fungistatic Activity of Modified Chitosans against *Saprolegnia parasitica*. *Biomacromolecules* **2001**, *2*, 165–169. [CrossRef]
24. El Hadrami, A.; Adam, L.R.; El Hadrami, I.; Daayf, F. Chitosan in Plant Protection. *Mar. Drugs* **2010**, *8*, 968–987. [CrossRef] [PubMed]
25. Liu, H.; Bao, J.; Du, Y.; Zhou, X.; Kennedy, J.F. Effect of Ultrasonic Treatment on the Biochemphysical Properties of Chitosan. *Carbohydr. Polym.* **2006**, *64*, 553–559. [CrossRef]
26. Kruk, T.; Szczepanowicz, K.; Stefańska, J.; Socha, R.P.; Warszyński, P. Synthesis and Antimicrobial Activity of Monodisperse Copper Nanoparticles. *Colloids Surf. B* **2015**, *128*, 17–22. [CrossRef] [PubMed]
27. Kanhed, P.; Birla, S.; Gaikwad, S.; Gade, A.; Seabra, A.B.; Rubilar, O.; Duran, N.; Rai, M. In vitro Antifungal Efficacy of Copper Nanoparticles against Selected Crop Pathogenic Fungi. *Mater. Lett.* **2014**, *115*, 13–17. [CrossRef]
28. Saharan, V.; Mehrotra, A.; Khatik, R.; Rawal, P.; Sharma, S.S.; Pal, A. Synthesis of Chitosan Based Nanoparticles and Their in vitro Evaluation against Phytopathogenic Fungi. *Int. J. Biol. Macromol.* **2013**, *62*, 677–683. [CrossRef]
29. Saharan, V.; Sharma, G.; Yadav, M.; Choudhary, M.K.; Sharma, S.S.; Pal, A.; Raliya, R.; Biswas, P. Synthesis and in vitro Antifungal Efficacy of Cu–Chitosan Nanoparticles against Pathogenic Fungi of Tomato. *Int. J. Biol. Macromol.* **2015**, *75*, 346–353. [CrossRef]
30. Nelson, P.E.; Toussoun, T.A.; Marasas, W.F.O. *Fusarium Species: An Illustrated Manual for Identification*; Pennsylvania State University Press: University Park, PA, USA, 1983.
31. Hirano, Y.; Arie, T. PCR-based differentiation of *Fusarium oxysporum* ff. sp. *lycopersici* and *radicis-lycopersici* and races of *F. oxysporum f.* sp. *lycopersici*. *J. Gen. Plant. Pathol.* **2006**, *72*, 273–283. [CrossRef]

32. Çolak, A.; Biçici, M. PCR detection of *Fusarium oxysporum f.* sp. *radicis-lycopersici* and races of *F. oxysporum f.* sp. *lycopersici* of tomato in protected tomato-growing areas of the eastern Mediterranean region of Turkey. *Turk. J. Agric. For.* **2013**, *37*, 457–467. [CrossRef]
33. Oh, J.-W.; Chun, S.C.; Chandrasekaran, M. Preparation and in vitro Characterization of Chitosan Nanoparticles and Their Broad-Spectrum Antifungal Action Compared to Antibacterial Activities against Phytopathogens of Tomato. *Agronomy* **2019**, *9*, 21. [CrossRef]
34. El-Abeid, S.E.; Ahmed, Y.; Daròs, J.-A.; Mohamed, M.A. Reduced Graphene Oxide Nanosheet-Decorated Copper Oxide Nanoparticles: A Potent Antifungal Nanocomposite against Fusarium Root Rot and Wilt Diseases of Tomato and Pepper Plants. *Nanomaterials* **2020**, *10*, 1001. [CrossRef]
35. Chen, J.; Peng, H.; Wang, X.; Shao, F.; Yuan, Z.; Han, H. Graphene oxide exhibits broad-spectrum antimicrobial activity against bacterial phytopathogens and fungal conidia by intertwining and membrane perturbation. *Nanoscale* **2014**, *6*, 1879–1889. [CrossRef]
36. Lichtenthaler, H.K. Chlorophylls and carotenoids: Pigments of photosynthetic biomembranes. In *Methods in Enzymology*; Academic Press: New York, NY, USA, 1987; Volume 148, pp. 350–382. [CrossRef]
37. Kim, S.W.; Jung, J.H.; Lamsal, K.; Kim, Y.S.; Min, J.S.; Lee, Y.S. Antifungal effects of silver nanoparticles (AgNPs) against various plant pathogenic fungi. *Mycobiology* **2012**, *40*, 53–58. [CrossRef] [PubMed]
38. Vetter, J.L.; Steinberg, M.P.; Nelson, A.L. Quantitative Determination of Peroxidase in Sweet Corns. *J. Agric. Food Chem.* **1958**, *6*, 39–41. [CrossRef]
39. Gorin, N.; Heidema, F.T. Peroxidase Activity in Golden Delicious Apples as a Possible Parameter of Ripening and Senescenc. *J. Agric. Food Chem.* **1976**, *24*, 200–201. [CrossRef] [PubMed]
40. Stangarlin, J.R.; Pascholati, S.F. Activities of Ribulose-1,5-Bisphosphate Carboxylase-Oxygenase (Rubisco), Chlorophyllase, _-1,3 Glucanase and Chitinase and Chlorophyll Content in Bean Cultivars (*Phaseolus vulgaris*) Infected with Uromyces Appendiculatus. *Summa Phytopathol.* **2000**, *26*, 34–42.
41. Ramírez, G.M.; Rojas, L.I.; Avelizapa, N.G.; Avelizapa, R.; Camarillo, R.C. Colloidal Chitin Stained with Remazol Brilliant Blue R, a Useful Substrate to Select Chitinolytic Microorganisms and to Evaluate Chitinases. *J. Microbiol. Methods* **2004**, *56*, 13–19.
42. Lopes, M.A.; Gomes, D.S.; Koblitz, M.G.B. Use of Response Surface Methodology to Examine Chitinase Regulation in the Basidiomycete Moniliophthora Perniciosa. *Mycol. Res.* **2008**, *112*, 399–406. [CrossRef]
43. Summerell, B.A.; Salleh, B.; Leslie, J.F. A utilitarian approach to Fusarium identification. *Plant Dis.* **2003**, *87*, 117–128. [CrossRef] [PubMed]
44. Booth, C. *The Genus Fusarium*; Commonwealth Mycological Institute: Kew, UK, 1971.
45. Murugan, L.; Krishnan, N.; Venkataravanappa, V.; Saha, S.; Mishra, A.K.; Sharma, B.K.; Rai, A.B. Molecular characterization and race identification of *Fusarium oxysporum f.* sp. *lycopersici* infecting tomato in India. *3 Biotech* **2020**, *10*, 486. [CrossRef]
46. Logpriya, S.; Bhuvaneshwari, V.; Vaidehi, D.; SenthilKumar, R.P.; Nithya Malar, R.S.; Sheetal, B.P.; Kalaiselvi, M. Preparation and characterization of ascorbic acid-mediated chitosan–copper oxide nanocomposite for anti-microbial, sporicidal and biofilm-inhibitory activity. *J. Nanostruct. Chem.* **2018**, *8*, 301–309. [CrossRef]
47. Awwad, A.M.; Albiss, B.A.; Salem, N.M. Antibacterial activity of synthesized copper oxide nanoparticles using Malva sylvestris leaf extract. *SMU Med. J.* **2015**, *2*, 91–101.
48. Syame, S.M.; Mohamed, W.S.; Mahmoud, R.K.; Omara, S.T. Synthesis of copper-chitosan nanocomposites and their applications in treatment of local pathogenic isolates bacteria. *Orient. J. Chem.* **2017**, *33*, 2959–2969. [CrossRef]
49. Hidangmayum, A.; Dwivedi, P. Chitosan based nanoformulation for sustainable agriculture with special reference to abiotic stress: A review. *J. Polym. Environ.* **2022**, *30*, 1264–1283. [CrossRef]
50. Singh, R.K.; Martins, V.; Soares, B.; Castro, I.; Falco, V. Chitosan application in vineyards (*Vitis vinifera* L. cv. Tinto Cão) induces accumulation of anthocyanins and other phenolics in berries, mediated by modifications in the transcription of secondary metabolism genes. *Int. J. Mol. Sci.* **2020**, *21*, 306. [CrossRef] [PubMed]
51. Xiong, L.; Tong, Z.H.; Chen, J.J.; Li, L.L.; Yu, H.Q. Morphology-dependent antimicrobial activity of Cu/Cu_xO nanoparticles. *Ecotoxicology* **2015**, *24*, 2067–2072. [CrossRef] [PubMed]
52. Giannousi, K.; Sarafidis, S.; Mourdikoudis, G.; Pantazaki, A.; Dendrinou-Samara, C. Selective synthesis of Cu2O and Cu/Cu2O NPs: Antifungal activity to yeast saccharomyces cerevisiae and DNA interaction. *Inorg. Chem.* **2014**, *53*, 9657–9666. [CrossRef] [PubMed]
53. Huang, S.; Wang, L.; Liu, L.; Hou, Y. Nanotechnology in agriculture, livestock, and aquaculture in China. "A review". *Agron. Sustain. Dev.* **2015**, *35*, 369–400. [CrossRef]
54. Khatami, M.; Varma, R.; Heydari, M.; Peydayesh, M.; Sedighi, A.; Askari, H.A.; Rohani, M.; Baniasadi, M.; Arkia, S.; Seyedi, F.; et al. Copper oxide nanoparticles greener aynthesis using tea and its antifungal efficiency on *Fusarium solani*. *Geomicrobiol. J.* **2019**, *36*, 777–781. [CrossRef]
55. Evans, I.; Solberg, E.; Huber, D.M. *Mineral Nutrition and Plant*; Datnoff, L.E., Elmer, W.H., Huber, D.N., Eds.; APS Press: St. Paul, MN, USA, 2007.
56. Snedecor, G.W.; Cochran, W.G. *Statistical Methods*, 7th ed.; Iowa State University Press: Ames, IA, USA, 1980.
57. Zhang, X.F.; Gurunathan, S. Biofabrication of a novel biomolecule-assisted reduced graphene oxide: An excellent biocompatible nanomaterial. *Int. J. Nanomed.* **2016**, *11*, 6635. [CrossRef] [PubMed]

58. Bondarenko, O.; Juganson, K.; Ivask, A.; Kasemets, K.; Mortimer, M.; Kahru, A. Toxicity of Ag, CuO and ZnOnanoparticles to selected environmentally relevant test organisms and mammalian cells in vitro: A critical review. *Arch. Toxicol.* **2013**, *87*, 1181–1200. [CrossRef] [PubMed]
59. Goyal, P.; Chakraborty, S.; Misra, S.K. Multifunctional Fe3O4-ZnO nanocomposites for environmental remediation applications. *Environ. Nanotechnol. Monit. Manag.* **2018**, *10*, 28–35. [CrossRef]
60. Dreyer, D.R.; Park, S.; Bielawski, C.W.; Ruo, R.S. The chemistry of graphene oxide. *Chem. Soc. Rev.* **2010**, *39*, 228–240. [CrossRef] [PubMed]
61. Karthik, R.; Govindasamy, M.; Chen, S.M.; Chen, T.W.; Elangovan, A.; Muthuraj, V.; Yu, M.C. A facile graphene oxide based sensor for electrochemical detection of prostate anti-cancer (anti-testosterone) drug flutamide in biological samples. *RSC Adv.* **2017**, *7*, 25702–25709. [CrossRef]
62. Raffi, M.; Mehrwan, S.; Bhatti, T.M.; Akhter, J.I.; Hameed, A.; Yawar, W. Investigations into the Antibacterial Behavior of Copper Nanoparticles against *Escherichia coli*. *Ann. Microbiol.* **2010**, *60*, 75–80. [CrossRef]
63. Raghunath, A.; Perumal, E. Metal oxide nanoparticles as antimicrobial agents: A promise for the future. *Int. J. Antimicrob. Agents* **2017**, *49*, 137–152. [CrossRef]
64. Priester, J.H.; Ge, Y.; Mielke, R.E.; Horst, A.M.; Moritz, S.C.; Espinosa, K.; Schimel, J.P. Soybean susceptibility to manufactured nanomaterials with evidence for food quality and soil fertility interruption. *Proc. Natl. Acad. Sci. USA* **2012**, *109*, E2451–E2456. [CrossRef]
65. Kalagatur, N.K.; Nirmal Ghosh, O.S.; Sundararaj, N.; Mudili, V. Antifungal activity of chitosan nanoparticles encapsulated with *Cymbopogon martinii* essential oil on plant pathogenic fungi *Fusarium graminearum*. *Front. Pharmacol.* **2018**, *9*, 610. [CrossRef]
66. Colman, S.L.; Salcedo, M.F.; Mansilla, A.Y.; Iglesias, M.J.; Fiol, D.F.; Martín-Saldaña, S.; Casalongué, C.A. Chitosan microparticles improve tomato seedling biomass and modulate hormonal, redox and defense pathways. *Plant Physiol. Biochem.* **2019**, *143*, 203–211. [CrossRef]
67. Arias, M.M.D.; Leandro, L.F.; Munkvold, G.P. Aggressiveness of Fusarium species and impact of root infection on growth and yield of soybeans. *Phytopathology* **2013**, *103*, 822–832. [CrossRef] [PubMed]
68. Elmer, W.H.; White, J.C. The use of metallic oxide nanoparticles to enhance growth of tomatoes and eggplants in disease infested soil or soilless medium. *Environ. Sci. Nano* **2016**, *3*, 1072–1079. [CrossRef]
69. Fernández, V.; Brown, P.H. From plant surface to plant metabolism: The uncertain fate of foliar-applied nutrients. *Front. Plant. Sci.* **2013**, *4*, 289. [CrossRef]
70. Paul, P.K.; Sharma, P.D. *Azadirachta Indica* Leaf Extract Induces Resistance in Barley against Leaf Stripe Disease. *Physiol. Mol. Plant Pathol.* **2002**, *61*, 3–13. [CrossRef]
71. Ali, S.; Ganai, B.A.; Kamili, A.N.; Bhat, A.A.; Mir, Z.A.; Bhat, J.A.; Tyagi, A.; Islam, S.T.; Mushtaq, M.; Yadav, P. Pathogenesis-Related Proteins and Peptides as Promising Tools for Engineering Plants with Multiple Stress Tolerance. *Microbiol. Res.* **2018**, *212*, 29–37. [CrossRef] [PubMed]
72. Siddaiah, C.N.; Satyanarayana, N.R.; Mudili, V.; Kumar Gupta, V.; Gurunathan, S.; Rangappa, S.; Huntrike, S.S.; Srivastava, R.K. Elicitation of Resistance and Associated Defense Responses in *Trichoderma Hamatum* Induced Protection against Pearl Millet Downy Mildew Pathogen. *Sci. Rep.* **2017**, *7*, 43991. [CrossRef]
73. Butt, U.R.; Naz, R.; Nosheen, A.; Yasmin, H.; Keyani, R.; Hussain, I.; Hassan, M.N. Changes in Pathogenesis-Related Gene Expression in Response to Bioformulations in the Apoplast of Maize Leaves against *Fusarium oxysporum*. *J. Plant Interact.* **2019**, *14*, 61–72. [CrossRef]
74. Nandakumar, R.; Babu, S.; Viswanathan, R.; Raguchander, T.; Samiyappan, R. Induction of Systemic Resistance in Rice against Sheath Blight Disease by *Pseudomonas Fluorescens*. *Soil. Biol. Biochem.* **2001**, *33*, 603–612. [CrossRef]
75. Ramamoorthy, V.; Samiyappan, R. Induction of Defence-Related Genes in Pseudomonas fluorescens—Treated Chilli Plants in Response to Infection by *Colletotrichum Capsici*. *J. Mycol. Plant Pathol.* **2001**, *31*, 146–155.
76. Ramamoorthy, V.; Raguchander, T.; Samiyappan, R. Enhancing Resistance of Tomato and Hot Pepper to Pythium Diseases by Seed Treatment with Fluorescent Pseudomonads. *Eur. J. Plant Pathol.* **2002**, *108*, 429–441. [CrossRef]
77. Chen, C.; Belanger, R.R.; Benhamou, N.; Paulitz, T.C. Defense Enzymes Induced in Cucumber Roots by Treatment with Plant Growth-Promoting Rhizobacteria (PGPR) and *Pythium Aphanidermatum*. *Physiol. Mol. Plant Pathol.* **2000**, *56*, 13–23. [CrossRef]
78. Conrath, U.; Pieterse, C.M.J.; Mauch-Mani, B. Priming in Plant–Pathogen Interactions. *Trends Plant Sci.* **2002**, *7*, 210–216. [CrossRef] [PubMed]